PROCEEDINGS OF SPIE

SPIEDigitalLibrary.org/conference-proceedings-of-spie

Temporal focusing-based multiphoton excitation fluorescence images with background noise cancellation via Hilbert-Huang transform

Yvonne Yuling Hu, Yuan-Rong Lo, Chun-Yu Lin, Chia-Yuan Chang, Shean-Jen Chen

Yvonne Yuling Hu, Yuan-Rong Lo, Chun-Yu Lin, Chia-Yuan Chang, Shean-Jen Chen, "Temporal focusing-based multiphoton excitation fluorescence images with background noise cancellation via Hilbert-Huang transform," Proc. SPIE 10883, Three-Dimensional and Multidimensional Microscopy: Image Acquisition and Processing XXVI, 108831C (21 February 2019); doi: 10.1117/12.2507695

SPIE.

Event: SPIE BiOS, 2019, San Francisco, California, United States

Temporal focusing-based multiphoton excitation fluorescence images with background noise cancellation via Hilbert-Huang transform

Yvonne. Yuling Hu[a], Yuan-Rong Luo[b], Chun-Yu Lin[c], Chia-Yuan Chang[d], Shean-Jen Chen[c,*]
[a]Department of Photonics, National Cheng Kung University, Tainan, Taiwan; [b]Department of Engineering Science, National Cheng Kung University, Tainan, Taiwan; cDepartment of Mechanical Engineering, , National Cheng Kung University, Tainan, Taiwan;[d]Institute of Imaging and Biomedical Photonics, College of Photonics, National Chiao Tung University, Tainan, Taiwan.

ABSTRACT

Temporal focusing multiphoton excitation microscopy has wide field-of-view and optical sectioning. By using digital micromirror device, it provides patterned illumination. However, without filling the back aperture of objective lens, the axial confinement is limited to micron-meters, leading the out-of-focus fluorophores excited and image blurred. In this study, Hilbert-Huang transform is proposed to reduce the background noise. The empirical mode decomposition is first applied to disassemble the image into intrinsic mode functions and then reconstruct by Hilbert transform after diminishing background residues. The axial confinement can be enhanced from 2.79 μm to 0.73 μm with structure frequency in 1.06 μm^{-1}.

Keywords: Temporal focusing; Digital micromirror device; Structured illumination microscopy; Hilbert-Huang transform

1. INTRODUCTION

Multiphoton excitation microscopy (MPE) using near-infrared wavelength has been widely used in biological research since its ability to generate fluorescence signals in deeper specimens. With pulsed laser and high numerical aperture (NA) objective lens, higher excitation photon fluence is reached in the focal points, generating nonlinear optical phenomenon in a micrometer level [1]. Based on this nonlinear scheme, two-photon excited fluorescence (TPEF) microscopy has deeper penetration depth and intrinsic optical sectioning, providing minimum invasiveness and lower photobleaching. With a three-axis point scanner, three-dimensional high spatial resolution fluorescence image can be reconstructed [2]. Furthermore, second harmonic generation (SHG) signal provides label-free imaging that reveals highly polarized molecules and non-centrosymmetric structures such as collagen and microtubules [3]. Therefore, MPE microscopy with TPEF and SHG is now a power tool for imaging thick tissues and in vivo studies. However, higher frame rate and/or high throughput method is needed for dynamic biological signals such as neuronal activities. Temporal focusing-based multiphoton excitation microscopy (TFMPEM) composed of a diffraction element and a 4-f system provides wide field-of-view TPEF imaging. The diffraction element, such as blazed grating, spatially disperses the ultrashort laser pulses into different angles according to the diffraction equation and thus broadens the laser pulse width. With a grating and a high NA objective lens including in the 4-f system, the dispersed spectral components will temporally overlap in phase at the focal plane of the objective lens, where the shortest pulse width is achieved and generate power to sufficiently excite the TPEF and SHG signals [4]. This temporal focusing configuration provides an axial excitation confinement (AEC) that only a few micrometers of depth of the specimen is excited. The excitation depth varies according to parameters including laser pulse width, initial beam size, optical magnification and the NA of objective lens [5]. TFMPEM with 3D wide-field excitation volume has been applied for fast Brownian motion tracking, wide-field fluorescence lifetime imaging and 3D neuronal activity [6-7]. Moreover, the high-throughput feature of TFMPEM has further been integrated with holographic optical tweezers and large-area multiphoton-induced ablation technique [8-9].

*sheanjen@nctu.edu.tw; phone +886-6-3032121 #57807; fax +886-6-3032535

Three-Dimensional and Multidimensional Microscopy: Image Acquisition and Processing XXVI, edited by Thomas G. Brown, Tony Wilson, Proc. of SPIE Vol. 10883, 108831C · © 2019 SPIE · CCC code: 1605-7422/19/$18 · doi: 10.1117/12.2507695

Structured illumination has been widely applied in images. By decomposing the illuminated frequency in the taken image, a higher lateral resolution image can be reconstructed. In TFMPEM, structured illumination allows not only enhancement in lateral resolution, the axial confinement is also depressed due to its optical property. TFMPEM with active spatial light modulator or digital micromirror device (DMD) as the optical mask is able to illuminate in arbitrary patterns, providing an alternative method for 3D lithographic microfabrication [10]. In principle, the fixed tilting angle of DMD is similar to the design of a blazed grating, which diffract the input light following the diffraction equation. Thus, the DMD is introduced to the TFMPEM as a substitution of blazed grating in which illumination pattern can be manipulated [11]. With the ability to produce patterns, it is also employed to improve the contrast and the quality of images. Various image reconstruction algorithm is thus developed in accordance of illuminating structures with different spatial frequency. Image deconvolution uses the point spread function (PSF) of the optical system to restore the distorted images that compromised by the image property and measurement imperfection [12]. Furthermore, an improved axial-resolved images can be rebuilt with a small number of patterned images in single sinusoidal spatial frequency. HiLo microscopy applies filters in one uniform image and one structured image to reconstruct a new image without out-of-focus noise [13]. Structured illumination microscopy (SIM) employs spatial modulation to expand the detectable frequency that limited by the detector and objective lens to achieve super-resolution image. Based on the nonlinear mechanism of fluorescence, nonlinear SIM (nSIM) can be applied with higher-order spatial frequency modulation to further broaden the detection bandwidth and improve both axial and lateral resolution [9].

However, the effective NA under the temporal focusing scheme is compromised due to its incapability of fulfilling the back focal plane of the objective lens, which enlarges the AEC to a few micrometers [14]. The widening of AEC excites not only the in-focus but also the out-of-focus molecules. The emission of out-of-focus fluorescence interferes with the desired signals, depriving the imaging contrast and the axial resolution. To solve this issue, HiLo has been adapted for decades to eliminate the background noise. However, manual filter design and parameter adjustment during image reconstruction are required, which makes it difficult to automate the process when it comes to 3D imaging. Hilbert transform is then used to replace HiLo algorithm [15]. Like HiLo, only two images with identical frequency but different phase are needed. This method discards the background information by subtracting one with the other and demodulates the structure on the images by Hilbert transform. However, the Talbot effect that induced by the introduction of DMD in a nonlinear scheme causes undesirable artifacts, which decreases the quality of reconstructed images. Therefore, a reconstruction method based on Hilbert-Huang transform (HHT) is adapted to reduce the background noise in this paper.

2. OPTICAL SETUP AND METHODS

2.1 Optical Setup of TFMPEM and System Calibration

Figure 1 shows a schematic diagram of the overall TFMPEM setup with a single DMD that functions as the blazed grating for spatial dispersion and simultaneous patterned illumination [11]. The ultrafast laser source is a Ti:Sapphire regenerative amplifier (Spitfire Pro XP, Spectra-Physics, USA) coupled with a Ti:Sapphire ultrafast oscillator (Tsunami, Spectra-Physics, USA) as the seed beam. The regenerative amplifier has a 10 kHz repetition rate with a center wavelength of 800 nm, and provides 400 μJ/pulse with a 90 fs pulse width. A combination of a half-wave plate (HWP) and polarization beam splitter (PBS) is adopted for power adjustment while maintaining horizontal polarization. The fast mechanical shutter (VS14S-2-ZM-0-R3, Uniblitz, USA) is open only when imaging is in progress to avoid unnecessary photobleaching. The DMD (DLP7000, Texas Instrument, USA) has a 0.7-inch illumination area and 1024 × 768 pixels in a diagonal micromirror array with 13.68 μm pitch size. The mechanical tilt angle of every micromirror element is ±12°, with + and – indicating reflecting (ON) and blocking (OFF) the incident laser beam, respectively. The structure of the DMD can be considered equivalent to a blazed grating with a blazed angle of 12°. Further, the 10th order diffraction of the ultrafast laser is adopted as the system beam, thereby approaching the maximum power set by the diffraction equation. The dispersion efficiency was verified as being equivalent to that when using the 1st order diffraction of a 517 lines/mm blazed grating [11]. Furthermore, the DMD can easily display 8-bit patterns via a high definition multimedia interface, and can also implement spatially modulated illumination in structured frequency and orientation; as such, it induces diverse diffraction effects in efficiency and orientation. Accordingly, the DMD in the system acts not only as a

dispersion element for temporal focusing, but also as a spatially modulated illuminator with diffraction effect at the back focal plane of objective.

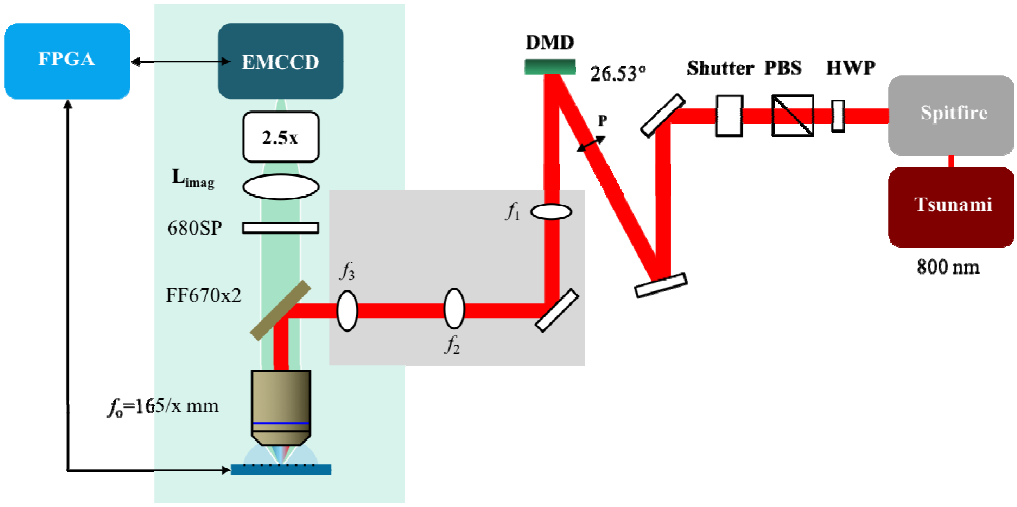

Figure 1. Optical setup of TFMPEM with a DMD functioning as a blazed grating.

In the figure, f_1 and f_2 comprise the relay set, and together with f_3 and the objective (UPlanSApo 60XW/NA 1.2,Olympus, Japan) f_o form the 4-f system for temporal focusing excitation in an upright optical microscope (Axio Imager.A2m, Carl Zeiss, Germany). The TPEF and SHG signal are first filtered by the dichroic mirror and short-pass filter to remove the reflected excitation laser, and then imaged to the high-sensitivity EMCCD (iXon Ultra 897, Andor, UK) through the L3 imaging lens and an additional 2.5x camera adaptor. The EMCCD has 512 × 512 active pixels with a 16 μm pixel size and can be thermoelectrically cooled to −80 °C with air. It provides 16-bit digitization resolution and a maximum 17 MHz readout rate. In addition, 3D images can be acquired by controlling the motorized stage (H101A ProScan, Prior Scientific, UK) via the 3-axis encoder and fast piezo focusing stage (NanoScanZ 200, Prior Scientific, UK) with a maximum 200 μm traveling range. All peripheral instrument communication and control are operated via a high-speed data acquisition card (PCIe-7842R, National Instruments, USA) with Virtex-5 LX50 FPGA by custom-made LabVIEW program. The DMD-based TFMPEM has an AEC of 2.79 um by measuring the axial intensity profile of a 200 nm-thick thin film spin-coated with Rhodamine 6G dye and estimating the full-width-half-maxima (FWHM) of the fitted profile.

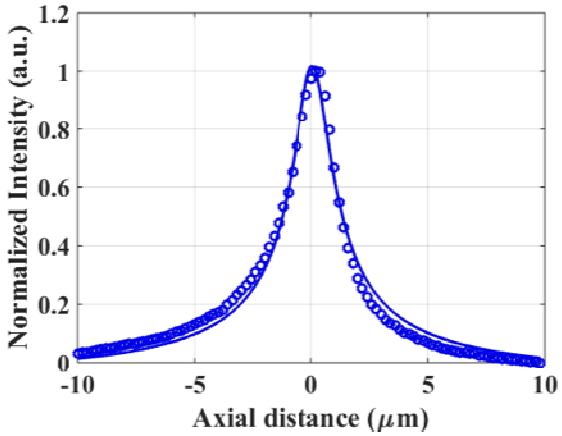

Figure 2. The intensity profile of the DMD-based TFMPEM system with 2.79 um in FWHM.

2.2 Hilbert-Huang Transform (HHT)

The Hilbert-Huang transform is an algorithm that decomposes the input signals before applying Hilbert transform (HT). In the beginning, the input signals are deciphered into multiple intrinsic mode functions (IMF) and a residual element by empirical mode decomposition (EMD) [16]. The early terms of IMF encode most of the high frequency information of the input signals, where the later terms and the residual elements encode the low frequency information including the background noise. After the decoupling, selective reconstruction (SR) is applied to diminish the noise. The filtered IMF is then demodulated using Hilbert transform. In order to process two-dimensional images, it is essential to extend EMD into bi-dimensional empirical mode decomposition (BEMD). However, it is time-consuming for BEMD to compute every single image. Therefore, enhanced fast empirical mode decomposition (EFEMD) is applied in order to reduce computation. A 3x3 mask is first applied to calculate the averaged local maxima and minima of the images, and n is then obtained by averaging the two values. A filter with diameter d is then designed, which d denotes the number of the square root of image size divided by n. The filter then portrays the local extrema of the image to produce the outfit of the signals. Afterwards, the shifting process of EMD is utilized for decomposition.

3. EXPERIMENTAL RESULTS AND DISCUSSION

3.1 HHT and Talbot effect

The 200 nm-thick R6G thin film is then again used to examine the algorithm. A 0°-oriented and a 90°-oriented sinusoidal patterns with 1.06 μm^{-1} in spatial frequency k_p are used in the structured illumination. HHT is then applied to remove background noise in every stack of image. The average intensity of each stack is then fitted by the axial resolution of temporal focusing as shown in Figure 3. After applying HHT, a better optical sectioning is achieved. The axial confinement is enhanced from 2.79 μm to 0.73. Furthermore, Talbot effect is found in the intensity profile of 90°-oriented pattern, which has an unusual sideband located in 0.4 μm away from focal point, as shown in Figure 3. The observed Talbot effect distance is considered an outcome of using DMD as blazed grating. Unlike a blazed grating, DMD is composed of 2-dimensional array of micromirror, which endowed DMD with polarization-independent property. However, when it comes to the nonlinear phenomenon, this advantage will then become a critical issue in pattern design. In two-photon excitation, the Talbot effect becomes more obvious when the orientation of the periodic pattern is orthogonal to the orientation of the spatial frequency of the diffraction component, which the frequency is unable to be compensated and the consequence of the pulse change is severed.

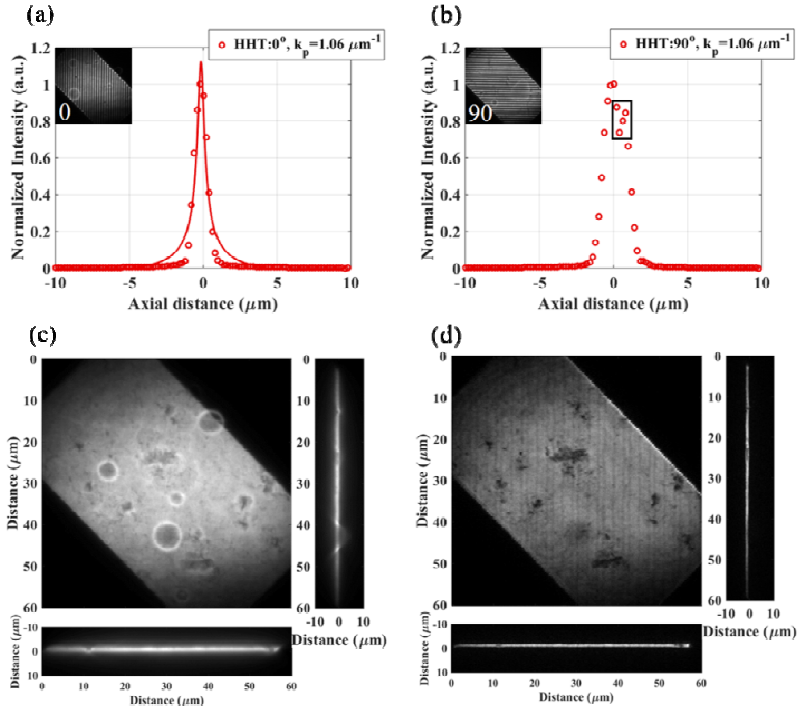

Figure 3. The effect of pattern orientation to the HHT-reconstructed images. (a)When the orientation of the periodic pattern is parallel to the orientation of DMD, no Talbot effect is observed, while (b) the orientation is orthogonal to the other, the Talbot effect will cause a sideband in the intensity profile. The Talbot effect will reduce the overall intensity of the reconstructed image as shown in (c) and (d) in respective.

3.2 Spatial frequency modulation

The modulation of spatial frequency of the periodic pattern is then considered for the deep tissue imaging. In order to realize the range of frequency this system can acquire with the pattern that DMD provides, 0°-oriented sinusoidal patterns with 0.31 μm^{-1}, 0.36 μm^{-1}, 0.53 μm^{-1} and 1.06 μm^{-1} in spatial frequency k_p are utilized to image the R6G thin film. The cutoff frequency is smaller when the distance from the focal plane get larger. Therefore, the background noise is less when the spatial frequency of the pattern is higher and thus enhance the optical sectioning.

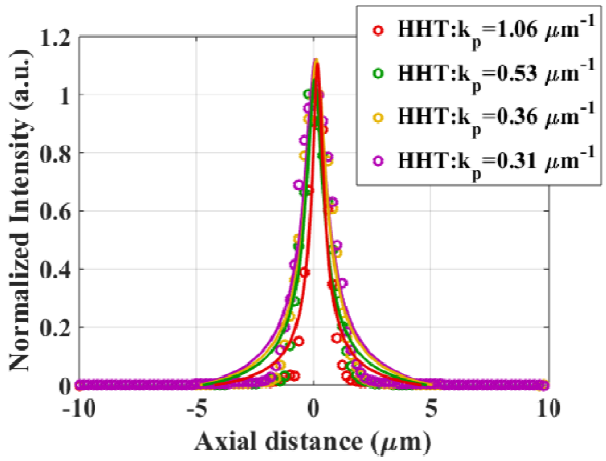

Figure 4. The axial intensity profile of the R6G thin film. The FWHM of 1.06 μm^{-1}, 0.53 μm^{-1}, 0.36 μm^{-1} and 0.31 μm^{-1} k_p are 0.73 μm, 1.08 μm, 1.22 μm, 1.37 μm respectively.

4. CONCLUSIONS

By utilizing DMD as diffraction component, the TFMPEM is not only able to achieve pattern illumination with precise phase projection, but also more tolerable from the air turbulence than the interferometric method, which allows HHT to accurately reconstruct the image without artifact. The DMD-based TFMPEM provides high-throughput excitation area, raise up the frame rate and reserve the advantage of low photodamage and deeper penetration. In order the enhance the axial confinement while retaining the high frame rate acquisition, HiLo which requires only two images are applied to reconstruct a TFMPEM image. However, the manually adjusted parameter will potential induce background difference, which results in the aliasing in the reconstructed images. HHT algorithm is then applied to rebuild the image automatically without producing residual. The overall axial confinement is enhanced from 2.79 μm to 0.73 μm.

REFERENCES

[1] Xu, C., Zipfel, W., Shear, J. B., Williams, R. M. and Webb, W. W., "Multiphoton fluorescence excitation: new spectral windows for biological nonlinear microscopy," Proc. Natl. Acad. Sci. U. S. A. 93(20), 10763-10768 (1996).
[2] Denk, W., Strickler, J. H. and Webb, W. W. "Two-photon laser scanning fluorescence microscopy," Science 248(4957), 73-76 (1990).
[3] Campagnola, P. J. and Loew, L. M, "Second-harmonic imaging microscopy for visualizing biomolecular arrays in cells, tissues and organisms," Nat. Biotechnol. 21, 1356–1360 (2003).

[4] Oron, D., Tal, E. and Silberberg, Y., "Scanningless depth-resolved microscopy," Opt. Express 13(5), 1468-1476 (2005).
[5] Dana, H. and Shoham, S., "Numerical evaluation of temporal focusing characteristics in transparent and applications," Opt. Express 19(6), 4937-4948 (2011).
[6] Cheng, L.-C., Chang, C.-Y., Lin, C.-Y., Cho, K.-C., Yen, W.-C., Chang, N.-S., Xu, C, Dong, C. Y. and Chen, S.-J., "Spatiotemporal focusing-based widefield multiphoton microscopy for fast optical sectioning," Opt. Express 20(8), 8939-8948 (2012).
[7] Schrödel, T., Prevedel, R., Aumayr, K., Zimmer, M., and Vaziri, A., "Brain-wide 3D imaging of neuronal activity in Caenorhabditis elegans with sculpted light," Nat. Methods 10(10), 1013–1020 (2013).
[8] Spesyvtsev, R., Rendall, H. A., and Dholakia, K., "Wide-field three-dimensional optical imaging using temporal focusing for holographically trapped microparticles," Opt. Lett. 40(21), 4847–4850 (2015).
[9] Lin, C.-Y., Li, P.-K., Cheng, L.-C., Li, Y.-C., Chang, C.-Y., Chiang, A.-S., Dong, C. Y., and Chen, S.-J., "High-throughput multiphoton-induced three-dimensional ablation and imaging for biotissues," Biomed. Opt. Express 6(2), 491–499 (2015).
[10] Li, Y.-C., Cheng, L.-C., Chang, C.-Y., Lin, C.-Y, Chang, N.-S., Campagnola, P. J., Dong, C. Y., and Chen, S.-J., "High-throughput fabrication of gray-level bio-microstructures via temporal focusing excitation and laser pulse control," J. Biomed. Opt. 18(7), 075004 (2013).
[11] Yih, J.-N., Hu, Y. Y., Sie, Y. D., Cheng, L.-C., Lien, C.-H. and Chen, S.-J., "Temporal focusing-based multiphoton excitation microscopy via digital micromirror device," Opt. Lett. 39(11), 3134–3137 (2014).
[12] Sarder, P. and Nehorai A., "Deconvolution methods for 3-D fluorescence microscopy images," IEEE Sig. Proc. Mag. 23(3), 32–45 (2006).
[13] Yew, E. Y. S., Choi, H., Kim, D. and So, P. T. C., "Wide-field two-photon microscopy with temporal focusing and HiLo background rejection," Proc SPIE, 7903, 79031O (2011).
[14] Choi, H., Yew, E. Y. S., Hallacoglu, B., Fantini, S., Sheppard, C. J. R. and So, P. T. C, "Improvement of axial resolution and contrast in temporally focused widefield two-photon microscopy with structured light illumination," Biomed. Opt. Express 4(7), 995–1005 (2013).
[15] Chang, C.-Y., Lin, C.-H., Lin, C.-Y., Sie, Y. D., Hu, Y. Y., Tsai, S.-F. and Chen, S.-J., "Temporal focusing-based widefield multiphoton microscopy with spatially modulated illumination for biotissue imaging," J Biophotonics. 11(1), e201600287 (2018).
[16] Meng, Y., Lin, W., Li, C. and Chen, S. C., "Fast two-snapshot structured illumination for temporal focusing microscopy with enhanced axial resolution," Opt. Express 25(19), 23109-23121 (2017).
[17] Trusiak, M., Wielgus M. and Patorski, K., "Advanced processing of optical fringe patterns by automated selective reconstruction and enhanced fast empirical mode decomposition," Opt Lasers Eng 52, 230-240 (2014).